The effect of degree of reduction on the electrical properties of functionalized graphene sheets

Cite as: Appl. Phys. Lett. **102**, 023114 (2013); https://doi.org/10.1063/1.4775582
Submitted: 29 October 2012 . Accepted: 17 December 2012 . Published Online: 18 January 2013

Christian Punckt, Franziska Muckel, Svenja Wolff, Ilhan A. Aksay, Carlos A. Chavarin, Gerd Bacher, and Wolfgang Mertin

The effect of degree of reduction on the electrical properties of functionalized graphene sheets

Christian Punckt,[1,2] Franziska Muckel,[1,3] Svenja Wolff,[1,3] Ilhan A. Aksay,[1,a)] Carlos A. Chavarin,[3] Gerd Bacher,[3,b)] and Wolfgang Mertin[3]
[1]*Department of Chemical and Biological Engineering, Princeton University, Princeton, New Jersey 08544, USA*
[2]*Vorbeck Materials Corp., 11 Deerpark Drive, Suite 203, Monmouth Junction, New Jersey 08852, USA*
[3]*Werkstoffe der Elektrotechnik and CENIDE, Universität Duisburg-Essen, 47057 Duisburg, Germany*

(Received 29 October 2012; accepted 17 December 2012; published online 18 January 2013)

We study the effect of carbon to oxygen ratio (C/O) on the electrical resistance of functionalized graphene sheets prepared by thermal exfoliation and reduction of graphite oxide at various temperatures. Using a 2-probe technique in conjunction with Kelvin probe force microscopy, we observe a transition from high-resistance (>400 kΩ/sq) nonlinear current/voltage characteristics at low C/O to low-resistance (<10 kΩ/sq) linear behavior at high C/O, indicating a transition from hopping to diffusive electron transport. Simultaneously, the metal-graphene contacts change from high-resistance Schottky-type behavior to nearly non-invasive metal-metal contact characteristics.
 [http://dx.doi.org/10.1063/1.4775582]

Functionalized graphene sheets (FGSs) produced by the thermal[1] or chemical[2] reduction of graphite oxide (GO) have recently found numerous applications in polymer composites,[3,4] electrical energy storage devices,[5–7] electrochemical sensors,[8–10] and photovoltaics.[11,12] What makes FGSs suitable for this wide range of uses is the fact that they combine electrical conductivity with a large number density of oxygen-containing functional groups and lattice defects (Fig. 1(a)).[13,14] In polymer composites, the presence of functional groups enhances load transfer between the polymer matrix and FGS filler through the formation of hydrogen bonds.[3] In electrochemical double layer capacitors, the presence of functional groups and defects provides a large electronic density of states which increases the surface-specific capacitance of FGSs by a factor of ∼3 compared to pristine (non-functionalized) graphene.[6] Electrochemical sensors and dye-sensitized solar cells rely on the electrocatalytic properties of functional groups and defects.[10,12]

Depending on synthesis method and resulting degree of reduction, a whole family of graphene materials can be fabricated with a broad spectrum of physical and chemical properties: On one end of the spectrum lies graphene oxide, a single layer of GO with a carbon to oxygen ratio (C/O) x between 1.8[15] and 2.3[16] depending on synthesis and characterization protocol.[16–18] Values of $x < 1.5$ have been reported in a small number of studies[19] and theoretical evidence exists that materials with such low C/O are thermodynamically stable.[20] However, such large degrees of oxidation may not be attainable in the experiment due to kinetic limitations.[21] Graphene oxide is an electrical insulator[22] since most of the carbon atoms in this material are sp^3-hybridized.[23,24] Pristine graphene lies on the other end of the spectrum of graphene materials and can, for example, be produced by chemical vapor deposition[25] or the so-called Scotch tape method.[26] It exhibits the smallest density of defects of all types of graphene and is practically free of oxygen-containing groups ($x \to \infty$). Its electronic properties have been studied in great detail,[27] revealing unprecedented charge carrier mobility in a carbonaceous material at room temperature[28,29] and, in the case of increased charge carrier density due to doping or application of bias, electrical sheet resistances $R_S \ll 1\,k\Omega/sq$.[30–32]

The electrical properties of graphene materials with intermediate C/O have been studied both by reducing individual sheets of graphene oxide on substrates and by oxidizing pristine graphene: Thermal and chemical reduction of graphene oxide sheets which were deposited on a substrate prior to reduction resulted in the onset of electrical conductivity.[22,24,33] Mildly reduced material was found to exhibit high resistance (hundreds of MΩ/sq to several hundred kΩ/sq) coupled with semiconducting behavior[34,35] and non-ohmic properties due to hopping effects[24,33] between sp^2-hybridized domains separated by non-reduced sp^3 areas.[33,36,37] Substrate-supported graphene oxide that was reduced strongly both chemically and, subsequently, thermally in an Ar/H_2 atmosphere at 900 °C showed low resistance (2.7 kΩ/sq) ohmic behavior[24] indicating that the properties of pristine graphene could partially be recovered. The transition from insulating to semiconducting to metallic behavior when proceeding from graphene oxide to highly reduced graphene is related to an increase of size and number of sp^2 domains with further reduction, until eventually a percolated sp^2 network forms within a background of sp^3 hybridized area at an oxygen content of about 10%.[36] Upon further reduction, hopping is no longer a dominating transport mechanism, and the diffusive motion of electrons is mostly limited by scattering at functional groups, lattice defects. Simultaneously, also the band gap decreases and metallic behavior begins to emerge.[34,35] Conversely, in studies based on the oxidation of pristine graphene, it has been shown that the introduction of functional groups and lattice defects, while providing benefits such as increased bonding to polymers and catalytic activity,

a)Author to whom correspondence should be addressed. Electronic mail: iaksay@princeton.edu.
b)Author to whom correspondence should be addressed. Electronic mail: gerd.bacher@uni-due.de.

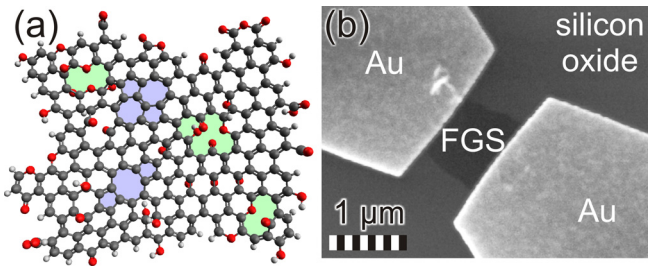

FIG. 1. (a) FGS schematic, (b) SEM image of a contacted graphene sheet.

at the same time decreases the electron mobility[38] and can induce semiconducting behavior.[35]

These studies provide insight into the relation between the physical and electrical properties of graphene materials. However, it has been shown that thermal processing of graphene on a silicon dioxide substrate—the typical choice for studies involving electrical characterization—yields results different from those obtained with freestanding graphene sheets.[39] For example, thermal treatment of graphene oxide on substrates has been shown to yield C/O of not more than 14.[40] FGSs fabricated in bulk amounts by the thermal exfoliation and reduction of GO powder (thus, in the absence of a substrate),[1] exhibit C/O between about 7 and 500,[41] depending on processing temperature and duration of the heat treatment. Thus, with thermally exfoliated FGSs we span almost the whole spectrum of graphene materials from graphene oxide to pristine graphene regarding their chemical composition, and their availability in bulk quantities makes it suitable for a wide range of applications. We denote our material as FGS_x where the subscript x represents the C/O, as defined above. The intrinsic electrical sheet resistance of thermally exfoliated FGSs (i.e., material that is not supported by a substrate during processing) has so far only been characterized for FGS_{20} exfoliated at 1050 °C, yielding values between 2.7 and 20 kΩ/sq determined by Kelvin probe force microscopy (KPFM) on only 3 individual sheets.[42] In order to understand the impact of FGSs in applications, however, it is necessary to know the electrical properties of the material as a function of processing conditions for a wide range of C/O.

Here, we present a systematic study of the electrical sheet resistance of FGSs exfoliated and reduced at various temperatures ranging from 500 °C ($FGS_{7.2}$) to 1500 °C (FGS_{340}) (see Table I) based on both I/V curves from 2-probe measurements (including contact resistance) and on KPFM (excluding contact resistance). We observe that with increasing x (decreasing oxygen content), the material undergoes a transition from high-resistance (>400 kΩ/sq for a C/O of 7.3) with pronounced non-ohmic current/voltage (I/V) characteristics to low resistance (less than 10 kΩ/sq for a C/O of 340) with ohmic behavior. Our measurements demonstrate that the electric conductivity of FGSs can be tuned in a wide range and, for the largest degree of reduction, by far exceeds the conductivity of chemically reduced graphene oxide and of graphene oxide reduced thermally on substrates.

GO was fabricated by oxidizing flake graphite powder (Asbury grade 3061) in an improved Hummers process.[24] FGSs were prepared by exfoliating and reducing the dry GO inside a tube furnace (Lindberg Blue M) for 60 s at various temperatures between 500 and 1100 °C under vacuum. To obtain more strongly reduced material, FGSs were either left inside the tube furnace for an extended period of time, or they were further annealed inside a graphite furnace (Astro1000, Thermal Technologies) under argon for one hour. The C/O of the resulting FGS powder was determined by combustion analysis (Atlantic Microlabs) and energy dispersive X-ray spectroscopy (EDS, INCA x-act, Oxford Instruments, attached to Vega 1 scanning electron microscope (SEM), Tescan USA) of compressed FGS pellets. A compilation of the produced materials is shown in Table I.

10 mm × 10 mm pieces of silicon wafer with a 300 nm top layer of thermally grown silicon oxide were used as substrates for electrical measurements. FGSs were suspended in ethanol at a concentration of 0.1 g/l by tip-sonication (Vibracell, Sonics & Materials Inc., CT) for 30 min, followed by centrifugation at 3000 rpm for 1 h (IEC Centra GP8R centrifuge with 218 A rotor). 10 ml of suspension was drop-cast onto the substrates and allowed to dry at room temperature overnight. The position of selected individual FGSs with respect to predefined alignment marks was measured with optical microscopy (Axioplan 2 with AxioCam HRc, Carl Zeiss MicroImaging, Inc.), and two electrical contacts were applied to each selected sheet using e-beam lithography (eLine, RAITH Inc.) and metal evaporation (Angstrom Engineering, ~10 nm Ti adhesion layer and ~100 nm Au) (Fig. 1(b)) followed by a lift-off.

In order to survey the electrical properties of a large number of FGSs prepared under different exfoliation and reduction conditions, their I/V characteristics were tested by applying voltages in the range from −1 to +1 V and recording the current flowing through the devices using a potentiostat (263 A, Princeton Applied Research) as power source. The topography of each sheet was determined with an atomic force microscope (AFM) in contact mode (Veeco Multimode with Nanoscope IIIa controller). The electrical resistance of the connection lines was determined independently and found to be insignificant (typically on the order of a few Ohms) compared to the resistance of the FGS and the metal/FGS contact (kΩ range).

In addition to the 2-probe method, single pass amplitude modulated KPFM was used in order to obtain the contact resistance at the metal/FGS interface as well as an independent measurement of intrinsic resistance for 6 additional FGSs with three different C/Os. The measurement setup and technique are described in detail elsewhere.[42–44] All electrical measurements were performed in air at room temperature.

The resistance of in total 25 FGSs was measured by recording I/V curves in a 2-probe configuration. The measurements for three representative FGSs are shown in Figure 2(a) and indicate the expected result that the current at a given applied voltage increases with increasing degree of reduction. We calculate an overall resistance R of the three devices of 750 ($FGS_{7.3}$), 162 (FGS_{24}), and 4.9 kΩ (FGS_{340}). After normalizing the I/V curves with respect to their slope at 0 V and plotting them on a linear scale (Fig. 2(b)), we find that the $FGS_{7.3}$ exhibits a non-linear I/V curve, while the measurements with more strongly reduced FGSs yield ohmic behavior (only shown for FGS_{24} in Figure 2(b)). Contact-mode AFM images of the contacted sheets are presented in Figures 2(c)–2(e). They show the

TABLE I. C/O of functionalized graphene exfoliated and annealed at various temperatures as used in this study. The specified errors represent the standard deviation between at least 5 measurements on each FGS powder.

Exfoliation	Annealing	C/O
500 °C, 60 s	…	7.3 ± 0.1
700 °C, 60 s	…	7.7 ± 0.7
900 °C, 60 s	…	9.9 ± 1.1
1100 °C, 60 s	…	24 ± 10
1100 °C, 10 min	…	65 ± 16
1100 °C, 60 s	1100 °C, 60 min (Ar)	170 ± 40
1100 °C, 60 s	1500 °C, 60 min (Ar)	340 ± 60

typical wrinkled morphology of functionalized graphene caused in part by the presence of functional groups and defects that induce strain in the carbon lattice[1,45] and likely also in part by drying phenomena (capillary forces) during the sheet deposition from the ethanol suspension. Based on the lateral dimensions of the area of the FGSs which is located in between the two gold contacts, we can estimate an "effective" sheet resistance $R_{S,eff}$ for the sheets, yielding values of 1170, 232, and 8.8 kΩ/sq. From the different average sheet thickness along cross sections through each of the sheets (Figs. 2(f)–2(h)), we conclude that the sheets are at multiple locations folded onto themselves[45] and likely do not represent single layer FGSs. Consequently, the single layer sheet resistance $R_{S,single}$ of the FGSs shown in Figures 2(c) and 2(e) is likely larger than the values of $R_{S,eff}$ specified above, as their average thicknesses are significantly larger than 2 nm indicating a multilayered structure.

However, during the measurement of a large number of sheets at each C/O, we observed that the scattering between values obtained from individual sheets of the same C/O batch is substantial (as previously observed in 4-probe measurements on substrate-reduced graphene oxide[24]), and that a thickness correction of the data does not have a significant influence on the calculated average values of $R_{S,single}$ if set into relation with the measurement error. The scattering of the data can be seen in the compilation of the results from the full data set of 25 sheets shown in Figure 3, where the error bars in the vertical direction represent the standard deviation of $R_{S,eff}$ (see Table II for numerical values) and horizontal error bars indicate standard deviation between several independent C/O measurements of the bulk powder. The large scattering of $R_{S,eff}$ is likely due to the combined effect of fluctuations in the degree of reduction of individual graphene sheets, variations in the sheet thickness (number of layers), and inaccuracies caused by non-negligible and varying contact resistance at the metal contact pads which cannot be excluded in a 2-probe measurement. (However, also in 4-probe measurements of graphene oxide reduced on substrates, large fluctuations were observed[24] although contact resistance effects were eliminated.) Despite the large scattering in the data for each C/O measured, a clear trend of decreasing $R_{S,eff}$ with increasing C/O can be observed in Figure 3, with the average sheet resistance falling by two orders of magnitude from a value of $R_{S,eff} \approx 500$ kΩ/sq for FGSs with C/O in the range from 7.3 to 9.9 to a value of $R_{S,eff} \approx 7.7$ kΩ/sq for a C/O of 340, individual sheets reaching $R_{S,eff} < 5$ kΩ/sq.

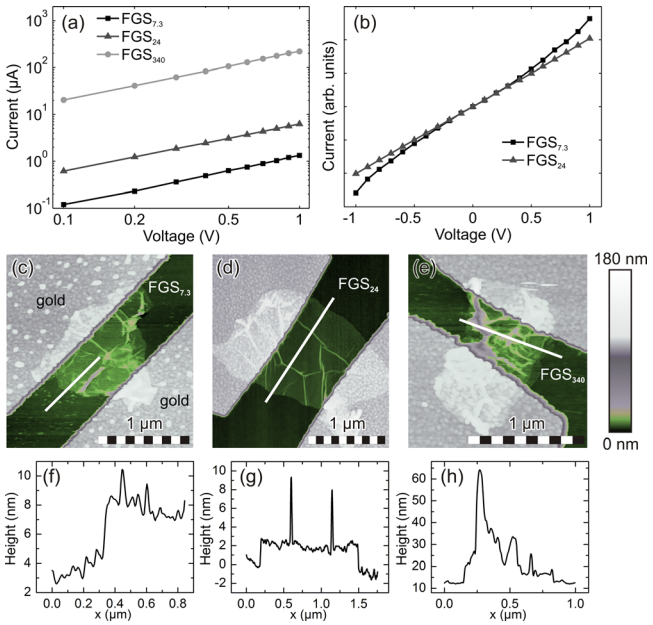

FIG. 2. (a) I/V curves for three representative FGSs. (b) Non-linear response of $FGS_{7.3}$ compared to linear response of FGS_{24}, curves are normalized with respect to the slope at 0 V. (c)–(e) AFM topography images of the FGSs corresponding to (a). (f)–(h) Cross-sections along the lines in (c)–(e).

In order to obtain information about the possible contribution of contact resistance to the data presented above and to test whether the non-ohmic behavior observed for low C/O sheets is a sheet-intrinsic phenomenon or perhaps is caused by the metal-graphene contact, we performed KPFM measurements on $FGS_{7.3}$, FGS_{24}, and FGS_{170}. As illustrated in Figure 4, where results from two sheets with C/O 7.3 and 24 are compared, we observe a qualitative difference between the KPFM measurements on $FGS_{7.3}$ and FGSs at larger C/O. The low-C/O FGSs exhibited a significant potential drop at the gold-FGS interface which appeared to be larger at the source (where the voltage was varied) than at the drain (held at ground potential at all times). Conversely, FGSs with larger C/O exhibited only a small potential drop at the metal contacts in accordance with our previous study.[42] In order to quantify the potential drops across contacts and FGSs, we calculated linear fit curves for the potential profiles in the contact and sheet regions (as shown in the lower part of Figure 4(a)) and determined potential differences by extrapolation to the edges of the gold contacts (dashed vertical lines in Figure 4(a)).

In Figure 5, we plot the device current as a function of the potential drops across source contact (V_S), graphene

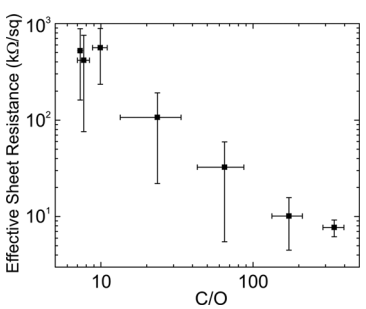

FIG. 3. Compilation of data from a total of 25 sheets measured with the 2-probe technique.

TABLE II. Sheet resistance measured by 2-probe technique and KPFM and contact resistances.

C/O	$R_{S,eff}$ (kΩ/sq)(2-probe)	$R_{S,eff}$ (kΩ/sq)(KPFM)	R_{Source}/R_{Drain} (kΩ)(KPFM)
7.3	520 ± 360	430	1000/148
7.7	420 ± 340	…	…
9.9	560 ± 330	…	…
24	110 ± 85	21	<1.6/1.9
65	32 ± 27	…	…
170	10.1 ± 5.6	8.7	<0.8/0.9
340	7.7 ± 1.5	…	…

sheet (V_{FGS}), and drain contact (V_D). This way, we obtain a set of three different I/V curves from each individual measurement that reflects the behavior of the contacts and the FGSs independently and that can be used to calculate the contact resistances as well as the effective sheet resistance of the FGSs. For $FGS_{7.3}$, we measured a pronounced non-ohmic relationship between current and V_{FGS}, V_{Drain}, and V_{Source}. The corresponding maximum effective sheet resistance is 430 kΩ/sq. The maximum contact resistances at source and drain were 1000 and 148 kΩ, respectively. A C/O of 7.3 corresponds to an oxygen content of 12%, and thus the sp^2 domains that have formed as a result of the thermal reduction treatment are likely not percolated.[36] Therefore, the observed non-linear intrinsic I/V curve is likely due to hopping within the FGSs, and we contend that the large contact resistance is related to semiconducting characteristics of the FGS resulting in a Schottky contact between the FGS and the metallic contact pad.[34,35] The asymmetry of the I/V curves obtained individually for source and drain contacts is not pronounced. For Schottky contacts, however, it is expected that while one contact is under reverse bias (high resistance) the other one should be under forward bias (low resistance) and vice versa, as the polarity of the source-drain voltage changes.[34] Since we do not find clear indication for such behavior in our data within the accuracy of our measurements, we conclude that the Schottky characteristics are superimposed by the onset of ohmic behavior and by convolution effects caused by the dimensions of the AFM tip, as demonstrated in a recent KPFM study of Si nanowire Schottky junctions.[46]

For the FGS_{24}, we find nearly linear I/V curves for sheet and contacts, corresponding to an intrinsic sheet resistance of 21 kΩ/sq. The contact resistances cannot be determined accurately due to the large noise in the voltage data. We estimate upper limits of 1.6 and 1.9 kΩ for source and drain contacts, respectively. Also, for FGSs with a C/O of 170, we measured a nearly ohmic I/V curve with KPFM, corresponding to an intrinsic resistance of typically a few kΩ and small contact resistances of less than 1 kΩ. These observations are attributed to the existence of a percolated network of sp^2 hybridized carbon within each FGS at this degree of reduction.[36] For all sheets characterized by KPFM, the overall device resistance corresponds, within measurement error, to the results from our 2-probe survey measurements. Our KPFM results in terms of sheet resistance and contact resistance are summarized and compared to the 2-probe data in Table II.

GO-derived graphene materials with an electrical conductivity comparable to that of our most strongly reduced

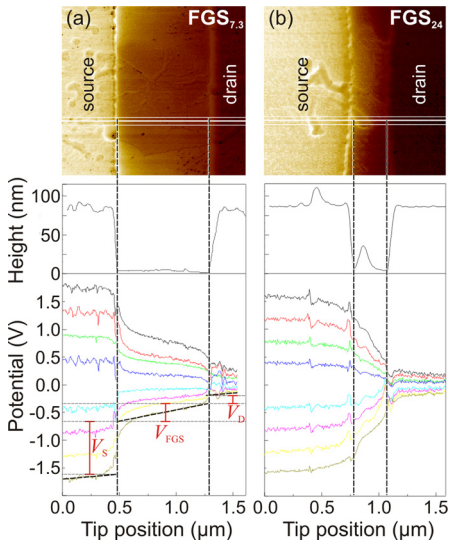

FIG. 4. KPFM data for two FGSs with C/O of (a) 7.3 and (b) 24. Top: Map of potential measured at a bias of +2 V. Bottom: Topography and potential profiles at applied voltages between +2 and −2 V along the indicated cross sections. Through linear fitting and extrapolation to the location of the gold contact edges (see dashed lines in the potential plot for (a)) the individual potential drops at source electrode (V_S), across the FGS (V_{FGS}) and at the drain electrode (V_D) are determined.

FGSs could, on a substrate, only be synthesized by a combination of chemical and subsequent thermal reduction at 900 °C in Ar/H_2.[24] Thermal reduction alone, without prior chemical treatment, cannot decrease the oxygen content of substrate-supported graphene oxide sufficiently[40] and thus yields resistances several orders of magnitude larger than those observed here. We suggest that in order to obtain resistances of 10 kΩ/sq and below, a sufficient reduction of both the oxygen content and the defect density is necessary. Thermally, this can only be achieved at temperatures in excess of 1000 °C at which the onset of structural changes in graphene has been observed.[47] Defects in the carbon backbone that emerge upon thermal reduction at lower temperatures, e.g., through the reduction of epoxide groups,[48,49] can be reduced in number through such thermal annealing.[47] Unlike in the case of substrate processing, with thermally exfoliated and reduced FGSs such high annealing temperatures can be achieved, resulting in the low observed resistances. We suspect that the combination of chemical and thermal reduction on a substrate yields high conductivities because the chemical reduction step likely results in either the absence or a largely decreased density of lattice defects compared to thermal

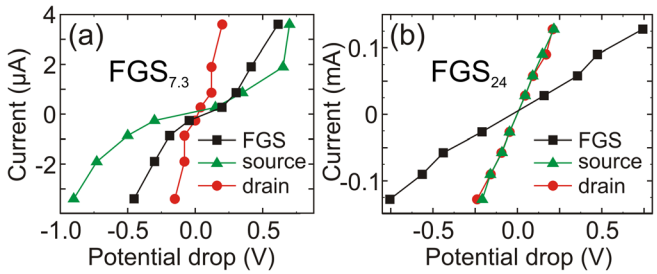

FIG. 5. I/V characteristics of FGSs and contacts as determined by KPFM, corresponding to the data shown in Figure 4. Device currents are plotted for (a) $FGS_{7.3}$ and (b) FGS_{24} as a function of the potential drops V_{FGS} across the FGSs (black squares) and as a function of the potential drops across source (V_S) and drain (V_D) contact for all applied voltages between +2 and −2 V.

TABLE III. Sheet resistance of different types of graphene.

Type	R_S (kΩ/sq)	Reference
FGS_7	~400	This work
FGS_{340}	~8	This work
Chemically reduced graphene oxide	>1000	33
Chemically + thermally reduced graphene oxide	2.7	24
Pristine graphene (no doping, no bias)	6.45	27–29
Pristine graphene (highly doped or biased)	<1	30 and 31
Pristine graphene (suspended, $n = 10^{12}\,cm^{-2}$)	0.028	32

reduction at temperatures up to 1000 °C. The subsequent thermal processing step probably yields C/O and defect densities comparable to the ones achieved in this study. A comparison of common types of graphene is shown in Table III.

In summary, we have shown that the thermal exfoliation and reduction of GO yield FGSs with a wide range of electrical properties, depending on exfoliation and reduction protocol. With increasing reduction time and temperature, we observed a transition from non-ohmic high-resistance (>400 kΩ/sq) to ohmic low-resistance (<10 kΩ/sq) behavior, achieving a minimum effective sheet resistance of 5 kΩ/sq for an individual sheet. Using KPFM, we were able to separate the contributions of intrinsic sheet resistance and contact resistance, showing that the observed non-linear I/V curves at low C/O are due to a combination of sheet intrinsic hopping-dominated charge transport and Schottky-type FGS-metal contacts.

The portion of the work at Princeton was supported by the Army Research Office (ARO)/Multidisciplinary Research Initiative (MURI) under Grant No. W911NF-09-1-476 and the Pacific Northwest National Laboratory (operated for the United States Department of Energy by Battelle) through Battelle Grant No. 66354. F.M. and S.W. acknowledge the SFB 445 of the Deutsche Forschungsgemeinschaft for the financial support. The work of C.A.C. was supported by The National Council on Science and Technology (CONACYT) Mexico under Grant No. 252826. We thank Michael A. Pope for assisting with FGS production.

[1]H. C. Schniepp, J. L. Li, M. J. McAllister, H. Sai, M. Herrera-Alonso, D. H. Adamson, R. K. Prud'homme, R. Car, D. A. Saville, and I. A. Aksay, J. Phys. Chem. B **110**, 8535 (2006).
[2]S. Stankovich, D. A. Dikin, R. D. Piner, K. A. Kohlhaas, A. Kleinhammes, Y. Jia, Y. Wu, S. T. Nguyen, and R. S. Ruoff, Carbon **45**, 1558 (2007).
[3]J. R. Potts, D. R. Dreyer, C. W. Bielawski, and R. S. Ruoff, Polymer **52**, 5 (2011).
[4]B. Ozbas, C. D. O'Neill, R. A. Register, I. A. Aksay, R. K. Prud'homme, and D. H. Adamson, J. Polym. Sci., Part B: Polym. Phys. **50**, 910 (2012).
[5]M. D. Stoller, S. J. Park, Y. W. Zhu, J. H. An, and R. S. Ruoff, Nano Lett. **8**, 3498 (2008).
[6]M. A. Pope, C. Punckt, and I. A. Aksay, J. Phys. Chem. C **115**, 20326 (2011).
[7]J. Xiao, D. H. Mei, X. L. Li, W. Xu, D. Y. Wang, G. L. Graff, W. D. Bennett, Z. M. Nie, L. V. Saraf, I. A. Aksay, J. Liu, and J. G. Zhang, Nano Lett. **11**, 5071 (2012).
[8]M. Zhou, Y. M. Zhai, and S. J. Dong, Anal. Chem. **81**, 5603 (2009).
[9]Y. Y. Shao, J. Wang, H. Wu, J. Liu, I. A. Aksay, and Y. H. Lin, Electroanalysis **22**, 1027 (2010).
[10]C. Punckt, M. A. Pope, J. Liu, Y. H. Lin, and I. A. Aksay, Electroanalysis **22**, 2834 (2010).
[11]J. D. Roy-Mayhew, D. J. Bozym, C. Punckt, and I. A. Aksay, ACS Nano **4**, 6203 (2010).
[12]J. D. Roy-Mayhew, G. Boschloo, A. Hagfeldt, and I. A. Aksay, ACS Appl. Mater. Interface **4**, 2794 (2012).
[13]K. N. Kudin, B. Ozbas, H. C. Schniepp, R. K. Prud'homme, I. A. Aksay, and R. Car, Nano Lett. **8**, 36 (2008).
[14]A. Bagri, C. Mattevi, M. Acik, Y. J. Chabal, M. Chhowalla, and V. B. Shenoy, Nat. Chem. **2**, 581 (2010).
[15]M. Hirata, T. Gotou, S. Horiuchi, M. Fujiwara, and M. Ohba, Carbon **42**, 2929 (2004).
[16]W. Scholz and H. P. Boehm, Z. Anorg. Allg. Chem. **369**, 327 (1969).
[17]O. C. Compton and S. T. Nguyen, Small **6**, 711 (2010).
[18]A. Dimiev, D. V. Kosynkin, L. B. Alemany, P. Chaguine, and J. M. Tour, J. Am. Chem. Soc. **134**, 2815 (2012).
[19]N. I. Kovtyukhova, P. J. Ollivier, B. R. Martin, T. E. Mallouk, S. A. Chizhik, E. V. Buzaneva, and A. D. Gorchinskiy, Chem. Mater. **11**, 771 (1999).
[20]J.-A. Yan, L. Xian, and M. Y. Chou, Phys. Rev. Lett. **103**, 086802 (2009).
[21]N. Lu, D. Yin, Z. Y. Li, and J. L. Yang, J. Phys. Chem. C **115**, 11991 (2011).
[22]I. Jung, D. A. Dikin, R. D. Piner, and R. S. Ruoff, Nano Lett. **8**, 4283 (2008).
[23]D. R. Dreyer, S. Park, C. W. Bielawski, and R. S. Ruoff, Chem. Soc. Rev. **39**, 228 (2010).
[24]D. C. Marcano, D. V. Kosynkin, J. M. Berlin, A. Sinitskii, Z. Z. Sun, A. Slesarev, L. B. Alemany, W. Lu, and J. M. Tour, ACS Nano **4**, 4806 (2010).
[25]X. S. Li, W. W. Cai, J. H. An, S. Kim, J. Nah, D. X. Yang, R. Piner, A. Velamakanni, I. Jung, E. Tutuc, S. K. Banerjee, L. Colombo, and R. S. Ruoff, Science **324**, 1312 (2009).
[26]K. S. Novoselov, A. K. Geim, S. V. Morozov, D. Jiang, Y. Zhang, S. V. Dubonos, I. V. Grigorieva, and A. A. Firsov, Science **306**, 666 (2004).
[27]A. H. Castro Neto, F. Guinea, N. M. R. Peres, K. S. Novoselov, and A. K. Geim, Rev. Mod. Phys. **81**, 109 (2009).
[28]K. S. Novoselov, A. K. Geim, S. V. Morozov, D. Jiang, M. I. Katsnelson, I. V. Grigorieva, S. V. Dubonos, and A. A. Firsov, Nature **438**, 197 (2005).
[29]A. K. Geim and K. S. Novoselov, Nat. Mater. **6**, 183 (2007).
[30]F. Schedin, A. K. Geim, S. V. Morozov, E. W. Hill, P. Blake, M. I. Katsnelson, and K. S. Novoselov, Nat. Mater. **6**, 652 (2007).
[31]J. H. Chen, C. Jang, S. D. Xiao, M. Ishigami, and M. S. Fuhrer, Nat. Nanotechnol. **3**, 206 (2008).
[32]E. V. Castro, H. Ochoa, M. I. Katsnelson, R. V. Gorbachev, D. C. Elias, K. S. Novoselov, A. K. Geim, and F. Guinea, Phys. Rev. Lett. **105**, 266601 (2010).
[33]C. Gomez-Navarro, R. T. Weitz, A. M. Bittner, M. Scolari, A. Mews, M. Burghard, and K. Kern, Nano Lett. **7**, 3499 (2007).
[34]X. S. Wu, M. Sprinkle, X. B. Li, F. Ming, C. Berger, and W. A. de Heer, Phys. Rev. Lett. **101**, 026801 (2008).
[35]S. N. Wang, R. Wang, X. W. Wang, D. D. Zhang, and X. H. Qiu, Nanoscale **4**, 2651 (2012).
[36]C. Mattevi, G. Eda, S. Agnoli, S. Miller, K. A. Mkhoyan, O. Celik, D. Mostrogiovanni, G. Granozzi, E. Garfunkel, and M. Chhowalla, Adv. Funct. Mater. **19**, 2577 (2009).
[37]K. Erickson, R. Erni, Z. Lee, N. Alem, W. Gannett, and A. Zettl, Adv. Mater. **22**, 4467 (2010).
[38]J. H. Chen, W. G. Cullen, C. Jang, M. S. Fuhrer, and E. D. Williams, Phys. Rev. Lett. **102**, 236805 (2009).
[39]S. Ryu, L. Liu, S. Berciaud, Y. J. Yu, H. T. Liu, P. Kim, G. W. Flynn, and L. E. Brus, Nano Lett. **10**, 4944 (2010).
[40]D. Yang, A. Velamakanni, G. Bozoklu, S. Park, M. Stoller, R. D. Piner, S. Stankovich, I. Jung, D. A. Field, C. A. Ventrice, and R. S. Ruoff, Carbon **47**, 145 (2009).
[41]J. Cao, G. Q. Qi, K. Ke, Y. Luo, W. Yang, B. H. Xie, and M. B. Yang, J. Mater. Sci. **47**, 5097 (2012).
[42]L. Yan, C. Punckt, I. A. Aksay, W. Mertin, and G. Bacher, Nano Lett. **11**, 3543 (2011).
[43]M. Nonnenmacher, M. P. Oboyle, and H. K. Wickramasinghe, Appl. Phys. Lett. **58**, 2921 (1991).
[44]T. Glatzel, S. Sadewasser, and M. C. Lux-Steiner, Appl. Surf. Sci. **210**, 84 (2003).
[45]H. C. Schniepp, K. N. Kudin, J. L. Li, R. K. Prud'homme, R. Car, D. A. Saville, and I. A. Aksay, ACS Nano **2**, 2577 (2008).
[46]E. Koren, N. Berkovitch, O. Azriel, A. Boag, Y. Rosenwaks, E. R. Hemesath, and L. J. Lauhon, Appl. Phys. Lett. **99**, 223511 (2011).
[47]J. Campos-Delgado, Y. A. Kim, T. Hayashi, A. Morelos-Gomez, M. Hofmann, H. Muramatsu, M. Endo, H. Terrones, R. D. Shull, M. S. Dresselhaus, and M. Terrones, Chem. Phys. Lett. **469**, 177 (2009).
[48]J. L. Li, K. N. Kudin, M. J. McAllister, R. K. Prud'homme, I. A. Aksay, and R. Car, Phys. Rev. Lett. **96**, 176101 (2006).
[49]R. Larciprete, S. Fabris, T. Sun, P. Lacovig, A. Baraldi, and S. Lizzit, J. Am. Chem. Soc. **133**, 17315 (2011).